Soluble ionic and oxygen isotopic compositions of a shallow firn profile, Baishui glacier No. 1, southeastern Tibetan Plateau

Hongxi PANG,[1] Yuanqing HE,[1,2] Wilfred H. THEAKSTONE,[3] David D. ZHANG[4]

[1]*Key Laboratory of Cryosphere and Environment, Cold and Arid Regions Environmental and Engineering Research Institute, Chinese Academy of Sciences, Lanzhou 730000, China*
E-mail: hx.pang@lzb.ac.cn
[2]*Institute of Tibetan Plateau Research, Chinese Academy of Sciences, Beijing 100085, China*
[3]*School of Environment and Development, University of Manchester, Manchester M13 9PL, UK*
[4]*Department of Geography, University of Hong Kong, Pokfulam Road, Hong Kong*

ABSTRACT. In the summer of 2004, a firn profile, 18.3 m long, extending down to glacier ice, was recovered in the accumulation area of the largest glacier, Baishui No. 1, on Yulong mountain, the southernmost glacier-covered area in mainland Eurasia. Multivariate empirical orthogonal function (EOF) and statistical correlation analyses of major-ion data from the profile demonstrate that three distinct types of ionic material contribute to the chemical characteristics of firn in this monsoonal region: material of marine origin, which is transported by the Indian southwest monsoon; crustal materials, which come from local sources; and anthropogenic pollutants, which are produced by industrial and agricultural activities in South Asia. Although the influence of post-depositional processes on the seasonal isotopic and soluble ionic compositions is significant, dust layers in the firn profile are clearly visible. Due to the effects of meltwater percolation, the dust layers generally coincide with late-summer snow surfaces. We therefore use the dust layers, combined with the seasonal variations of electrical conductivity (EC), Ca^{2+} and Mg^{2+}, to establish a depth/age scale for the firn profile. The reconstructed net accumulation has a significant negative correlation with the temperature at Lijiang, whereas the correlation between the net accumulation and the precipitation amount at Lijiang is weak. Although the $\delta^{18}O$ time series of the firn profile was modified significantly by meltwater percolation, the correlation between annual mean $\delta^{18}O$ values and the Indian southwest monsoon index (WSI1) is significant. This result suggests that $\delta^{18}O$ records from monsoon-influenced temperate glaciers can provide a valuable record of past variations of the Indian southwest monsoon.

1. INTRODUCTION

The world's polar ice sheets and ice caps are recognized as valuable archives of ambient atmospheric conditions, and they contain a unique record of climatic and environmental change. Snow, firn and ice samples recovered from low-latitude/high-altitude glaciers also have the potential to provide detailed paleo-environmental information (Schotterer and others, 1977; Stichler and others, 1982; Wagenbach, 1989; Koerner, 1997), although post-depositional processes may modify both isotopic and major-ion records. The recovery and analysis of snow and ice samples from appropriately located snow pits and ice cores has proved extremely valuable in producing continuous records of atmospheric chemistry and climate (Aizen and others, 1996; Kreutz and others, 2001; Hou and others, 2003; Nakazawa and others, 2004). The vast extent of glacierized regions in the high mountains of the Tibetan Plateau provides several suitable locations from which to recover glaciochemical records. Although glaciochemical investigations have been undertaken in the high mountains of the Tibetan Plateau, the existing dataset is limited spatially, especially in the region of the southeastern Tibetan Plateau.

Yulong mountain, located in the Hengduan range (southeastern edge of the Tibetan Plateau), north of Lijiang, Yunnan province, China, (27°10′–27°40′ N, 100°07′–100°10′ E) is the southernmost glacierized area in mainland Eurasia (Fig. 1). The largest glacier, Baishui glacier No. 1 (BG1), has an area of 1.52 km^2 and is 2.7 km long. Its broad, flat accumulation area covers about 1.0 km^2 at 4800–5000 m a.s.l. Meteorological conditions on Yulong mountain, responsible for the modern temperate glacier regime, are dominated by the South Asian/Indian monsoon in summer and by the southern branch of the westerlies in winter (Fig. 1). Seventy percent of the region's precipitation

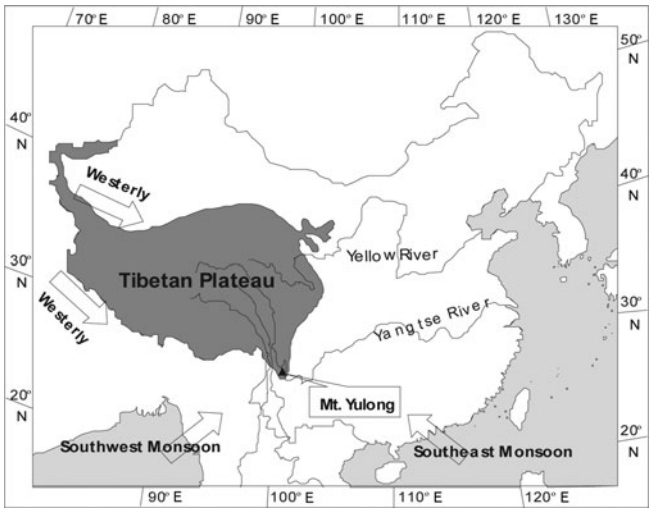

Fig. 1. Regional map of the Tibetan Plateau. The triangle represents the location of Yulong mountain.

https://doi.org/10.3189/172756407782871648 Published online by Cambridge University Press

Fig. 2. Photo of the location of the firn profile from the accumulation zone of BG1 at 4900 m a.s.l. Dust layers in the firn profile are clearly visible. Arrow indicates the sampling site.

falls between June and September from warm, moisture-rich air masses associated with the prevailing southwestern summer monsoon from the Indian Ocean. In winter, the climate is relatively dry, controlled by the winter monsoon of more proximal continental origin. As a result, both marine aerosols transported inland with the Asian monsoon and dust transported with the winter monsoon from the vast arid and semi-arid regions of central Asia contribute to glaciochemical records from the region.

Previous studies on Yulong mountain included retrieval of a firn core in summer 1999 (He and others, 2001, 2002). However, this firn core (10.1 m long) was rather shallow, and the glaciochemical information derived from it is limited. Moreover, there are few studies of the origin of the chemical composition of snow or firn on Yulong mountain. In July 2004, a longer natural firn profile (18.3 m long) was recovered from the accumulation zone of BG1 at 4900 m a.s.l. Our goals in this paper are to (1) investigate the origin of chemical constituents in the firn on Yulong mountain, and (2) reconstruct glaciochemical records from this firn profile.

2. METHODOLOGY

In order to investigate the glaciochemical characteristics in the region, and explore the relationship between preserved glaciochemistry and climatic processes, and the potential for recovering a longer time-series glaciochemical record from the Yulong mountain region, we visited BG1 in July 2004. Workers wearing non-particulating clean suits, masks and plastic gloves accessed the natural firn profile using a soft ladder (Fig. 2) and sampled it at 10 cm intervals. The outer layer of the profile (about 1.0 m thick) was removed prior to sampling to avoid the effects of contamination of the exposed surface. Samples were placed in pre-cleaned low-density polyethylene containers that had been washed by soaking and rinsing with 18.2 MΩ water. All samples were transported frozen to Lanzhou for chemical analysis at the Key Laboratory of Cryosphere and Environment. Analyses of stable oxygen isotope ratios ($\delta^{18}O$) were performed using a Finnigan delta-plus mass spectrometer (accuracy 0.05‰), and results are expressed relative to Standard Mean Ocean Water (SMOW). Samples were melted immediately prior to analysis for water-soluble inorganic ion content. Anion (Cl^-, NO_3^-, SO_4^{2-}) and cation (Na^+, Ca^{2+}, K^+, Mg^{2+}, NH_4^+) analyses were performed by ion chromatography (Dionex-300). The chromatography conditions were as follows: for cations, CS12 analytical column, 22 mM methanesulfonic acid (MSA) eluent and cation self-regenerating suppressor; for anions, AS4A-GC analytical column, 1.7 mM $NaHCO_3$/1.8 mM Na_2CO_3 eluent and anion self-regenerating suppressor. The analytical precision for each ion is 1 $\mu g\,L^{-1}$. After melting and warming to 20°C (room temperature), snow and ice samples were analyzed immediately for pH and electrical conductivity (EC) by a pH meter (PHJS-4A) (0–14 measurement range with uncertainty <1‰) and a conductivity meter (DDSJ-308A) (0–999 $\mu S\,cm^{-1}$ measurement range with an uncertainty <1‰) respectively. For each measurement, the electrode was calibrated with pH 6.86 and pH 9.18 reference buffers; the electrode was rinsed with deionized water after each sample, and the temperature-compensated pH determination was made on a fresh, quiescent sample after 5 min.

3. RESULTS AND ANALYSES

3.1. Ionic analysis

Mean ion concentrations in the firn profile are given in Table 1. To compare the relative contribution of each species to the overall chemical loading, the percentage of the total ionic charge was calculated on a sample-by-sample basis and averaged for the entire profile (Table 1). The dominant cation is Ca^{2+}, and Cl^- is the dominant anion analyzed. However, bicarbonate was not analyzed, and charge-balance considerations suggest that it is probably the dominant anion present. The average Cl^-/Na^+ ratio (calculated on a sample-by-sample basis and then averaged for the entire profile) is 1.9, similar to that of sea salt, which demonstrates that both ions have a dominantly marine source. Table 2 shows the correlation coefficients between soluble-ion species. Na^+ has particularly significant correlations with K^+ and Cl^-; NH_4^+ correlates significantly with SO_4^{2-}, K^+ and NO_3^-; Mg^{2+} with Ca^{2+}, EC and pH; and Ca^{2+} with EC and pH. Ca^{2+} and Mg^{2+} correlate most strongly with EC and pH, because Ca^{2+} is the dominant ion and limestone is the most abundant lithology in the region and a major source of alkalinity (Li and Su, 1996). Empirical orthogonal

Table 1. Summary of major-ion concentrations in the firn profile from Yulong mountain

	Ca^{2+}	Na^+	K^+	NH_4^+	Mg^{2+}	Cl^-	SO_4^{2-}	NO_3^-
Mean ($\mu g\,L^{-1}$)	595.0	58.3	33.4	92.5	41.5	79.3	51.3	63.5
%	50.7	6.7	4.2	12.0	4.0	10.0	6.0	6.4

https://doi.org/10.3189/172756407782871648 Published online by Cambridge University Press

Table 2. Correlation coefficients between soluble-ion species in the firn profile from Yulong mountain

	Na^+	NH_4^+	K^+	Mg^{2+}	Ca^{2+}	Cl^-	NO_3^-	SO_4^{2-}	pH	EC
Na^+	1	0.04	0.62[a]	0.06	0.11	0.61[a]	–0.00	0.18[b]	0.31[a]	0.19[b]
NH_4^+		1	0.41[a]	–0.11	0.02	0.13	0.18[b]	0.43[a]	–0.05	0.18[b]
K^+			1	–0.02	0.08	0.57[a]	–0.07	0.26[a]	0.13	0.20[b]
Mg^{2+}				1	0.77[a]	–0.10	0.14	–0.06	0.55[a]	0.67[a]
Ca^{2+}					1	0.03	0.17[b]	0.03	0.61[a]	0.89[a]
Cl^-						1	–0.05	0.18[b]	0.00	0.12
NO_3^-							1	0.23[b]	0.30[a]	0.22[b]
SO_4^{2-}								1	0.12	0.10
pH									1	0.54[a]
EC										1

[a]Correlation significant at the 0.01 confidence level. [b]Correlation significant at the 0.05 confidence level.

function (EOF) analysis of the eight major ions (Ca^{2+}, Mg^{2+}, Na^+, K^+, NH_4^+, SO_4^{2-}, NO_3^- and Cl^-) was used to detect a common structure within the multiple records (Meeker and others, 1995) (Table 3).

EOF1 accounts for 27.4% of the total variance in the major-ion series, is loaded with Na^+, Cl^- and K^+ and represents ionic material of marine origin. The good correlations between them also indicate that they derive from the common source.

Mg^{2+} and Ca^{2+} dominate EOF2, which accounts for 22.3% of the total variance and represents a terrestrial source. Previous studies also show high calcium and magnesium concentrations in snow, snow pits and ice cores from the southeastern Tibetan Plateau (Wake and others, 1993; Kang and others, 2000), reflecting a continental source from the arid regions of central Asia. However, the anomalously high calcium concentration compared with other chemical constituents (Table 1) indicates that the calcium is derived mainly from local limestone sources (Li and Su, 1996).

EOF3, loaded with NH_4^+, is probably related to biogenic material derived from regional agricultural activities (Shrestha and others, 1997; Kang and others, 2000; Hou and others, 2003). NO_3^- and SO_4^{2-} dominate EOF4 and EOF5 respectively. Both SO_4^{2-} and NO_3^- correlate poorly with Ca^{2+} and Mg^{2+} (Table 2), which suggests that the origin of Ca^{2+} and Mg^{2+} is different to that of NO_3^- and SO_4^{2-}. With the development of industry in South Asia, the contribution of the industrial exhaust gases (SO_2 and NO_x) to air pollution is significant. It has been reported that over 60% of the sulfur deposited in Nepal is derived from Indian emissions (Arndt and others, 1998), suggesting that the impact of long-range transport on pollutant deposition over other areas is significant. NO_3^- and SO_4^{2-} in the Yulong mountain area may therefore originate from industrial sources in South Asia. In addition, it has been reported that widespread biomass burning (firewood) for domestic energy in Nepal cannot be ignored as a source of NO_3^- and SO_4^{2-} (Davidson and others, 1986). NH_4^+ correlates well with SO_4^{2-} and NO_3^- (Table 2), suggesting that the three ions are co-deposited as ammonium sulfate and ammonium nitrate salts (Jang and others, 2002).

In summary, NH_4^+, SO_4^{2-} and NO_3^- in the Yulong mountain area probably derived from anthropogenic sources, and are transported to the area by the Indian southwest monsoon in summer and by the south branch of the westerlies in winter.

3.2. Firn profile dating

High ice temperatures, intense melting, rapid ice movement and high sensitivity to climate change characterize the temperate glaciers in the Yulong mountain region (Li and Su, 1996). According to observations made at about 4800 m on the glacier by Su and Wang (1996) between June and July 1982, the temperature was close to the melting point in the uppermost 2 m of snow, but decreased to below 0°C between 2.0 and 8.2 m depth. There was a slight increase below 8.2 m. These observations indicate the influence of meltwater percolation in the uppermost 2.0 m is obvious. Although the deeper firn was once close to the surface and it had been affected by meltwater percolation at that time, after that it was probably less affected by meltwater percolation due to a relatively low temperature. The glacier consists of two zones from terminus to summit: the ablation zone and the infiltration–congelation zone (Shi and others, 1988). The sampling site is in the infiltration–congelation zone.

In the region of the southeastern Tibetan Plateau, seasonal changes of dust transportation cause the highest Ca^{2+} and Mg^{2+} concentrations in the troposphere to occur in spring (Kang and others, 2000). Over the course of the ablation season, dust deposited in spring snow is concentrated on the late-summer ablation surface. The locations of summer surfaces can thus be identified on the basis of the distribution of dust layers, and these layers can therefore be used to date the firn profile. In addition, soluble ionic composition at dust layers is also higher than that at non-dust layers because soluble impurities are probably

Table 3. EOF analysis of the major-ion time series of the firn profile

	EOF1	EOF2	EOF3	EOF4	EOF5
Na^+	0.895	–0.083	0.097	–0.013	–0.087
NH_4^+	0.069	0.037	–0.939	–0.081	–0.233
K^+	0.786	–0.024	–0.468	–0.061	0.008
Mg^{2+}	–0.030	–0.940	0.079	–0.046	0.042
Ca^{2+}	0.064	–0.935	–0.043	–0.079	–0.023
Cl^-	0.862	0.057	–0.041	0.065	–0.103
NO_3^-	–0.018	–0.105	–0.080	–0.984	–0.108
SO_4^{2-}	0.140	0.018	–0.223	–0.116	–0.953
Total (%)	27.4	22.3	14.7	12.6	12.4

https://doi.org/10.3189/172756407782871648 Published online by Cambridge University Press

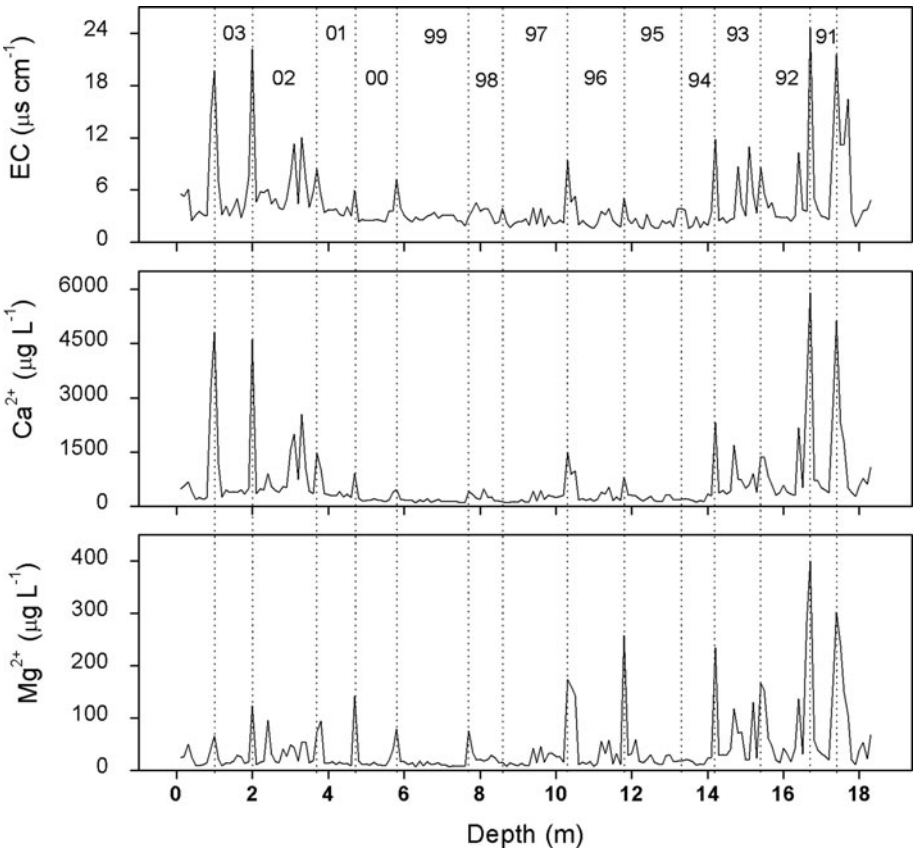

Fig. 3. EC, Ca^{2+} and Mg^{2+} records in the BG1 firn profile. The firn profile was dated using the peaks of EC, Ca^{2+} and Mg^{2+} in the firn profile. The dot lines generally correspond to the locations of dust layers in the firn profile recorded during sampling. The number 03 represents the period October 2002–September 2003, the number 02 the period October 2001–September 2002, etc.

deposited synchronously with dust. Therefore EC (representing the total ion load) peaks in the firn profile are consistent with the dust layers recorded during sampling. The peaks of EC, Ca^{2+} and Mg^{2+} were used to date the firn profile because EC correlated well with Ca^{2+} and Mg^{2+}. Each peak corresponds to a well-preserved dust layer on the late-summer snow surface. Therefore the snow accumulated between two peaks of EC (Ca^{2+}, Mg^{2+}) represents the net accumulation of snow within a balance year (October to the following September). Based on this dating, 13 complete annual layers were identified (Fig. 3). Identification of the years 2002 and 1993 may seem unconvincing because there are two additional significant EC (Ca^{2+}) peaks within these identified years. However, there are no significant additional Mg^{2+} peaks within these years (Fig. 3). According to our field observations, the two additional EC (Ca^{2+}) peaks correspond to two thin ice layers that may have formed by meltwater refreezing during late summer. Elution of soluble ions may be hindered at the level of these ice layers, resulting in EC (Ca^{2+}) peaks. It has been reported that Mg^{2+} can be eluted more easily than other ions (Iizuka and others, 2002), so this may explain the absence of Mg^{2+} peaks at these levels. We therefore believe that the years 2002 and 1993 have been reliably identified. Additionally, the boundaries between the identified years 1997/98 and 1994/95 are not obvious. There are no peaks of Ca^{2+} and Mg^{2+} at the boundaries (Fig. 3), but there are two weak EC peaks that were used to separate the years 1997/98 and 1994/95. Thus there is probably little error in defining the years 1994, 1995, 1997 and 1998.

3.3. Firn profile records

Because of the very difficult conditions under which the firn profile was sampled, the density of the firn profile was not measured. In order to reconstruct the net accumulation, density data from the 10.1 m firn core recovered in 1999 were used (He and others, 2001, 2002). For the 1999 core, the density was measured at 10 cm intervals. From the surface to the depth 10.3 m of the 2004 firn profile, seven complete annual layers (1997–2003) were identified (Fig. 3). For each identified year, there are two boundary depths of the 2004 firn profile which were used to identify the year. The mean density of firn between two boundary depths of the 2004 firn profile was replaced by the mean density of firn between the same two depths of the 1999 core. For the identified year 1997, the mean density value between the two depths 8.6 and 10.3 m (the two boundary depths which were used to identify the year 1997) of the 2004 firn profile was replaced by the mean density value between the depths 8.6 and 10.1 m of the 1999 core. From 10.4 to 18.3 m depth of the 2004 firn profile, the uniform density 0.8 g cm^{-3} was used, because the firn below 10.3 m depth is close to ice. Therefore the density values for the 13 identified years were calculated based on the density data of the 1999 core. The net accumulation time series can also be reconstructed. Long time series of meteorological observations have not been made in the high-altitude Yulong mountain area. In order to study the influence of meteorological conditions on the net accumulation of snow at BG1, meteorological data from Lijiang, 25 km to the south, were used. Figure 4 shows

https://doi.org/10.3189/172756407782871648 Published online by Cambridge University Press

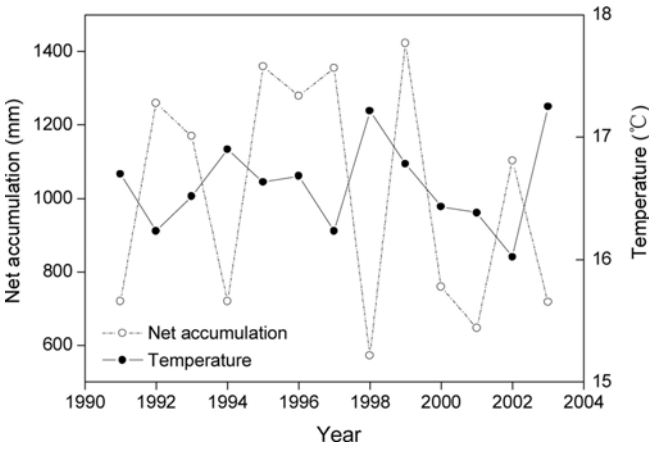

Fig. 4. The reconstructed net accumulation in the accumulation zone of BG1 and the mean temperature during the melting period (May–October) at Lijiang, 1991–2003.

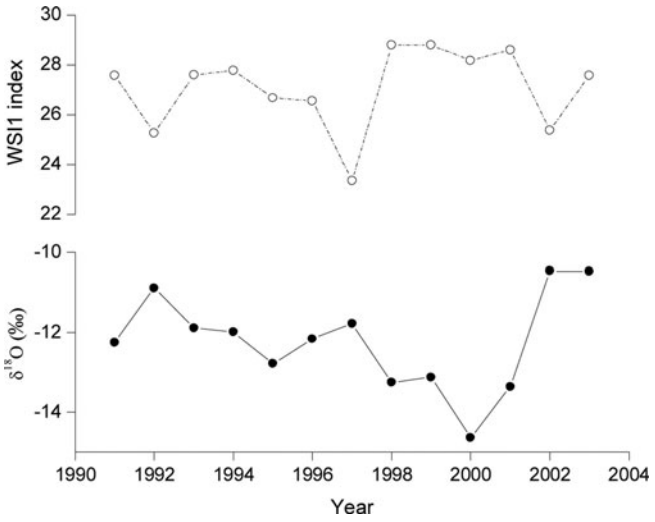

Fig. 5. Variations of the WSI1 index and the $\delta^{18}O$ record of the firn profile on Yulong mountain, 1991–2003. The negative correlation between them is significant.

the reconstructed net accumulation at the accumulation zone of BG1 and the mean temperature of the melting period (May–October) at Lijiang from 1991 to 2003. It is obvious that there is a negative correlation ($r = -0.46$, $p = 0.1$) between them, suggesting the temperature during the melting period plays an important role in net accumulation. Additionally, the correlation between the net accumulation and precipitation at Lijiang (not plotted in Fig. 4) was analyzed, but the correlation between them is very weak. The correlation between the reconstructed net accumulation and the temperature is not significant at the 0.05 confidence level nor is the correlation with precipitation, which may be caused by the following two reasons. Firstly, the effects of precipitation and temperature on the net accumulation may be counteracted partially. Secondly, the densities of samples from the 2004 firn were not measured, but inferred from measurements on the 1999 ice core. Some error in the reconstructed net accumulation could be introduced by the density data. The correlation between temperature and the net accumulation is more obvious than that between precipitation and the net accumulation, probably indicating that the net accumulation is more sensitive to temperature than to precipitation in the temperate glacier area under the global warming condition.

The seasonal variation in the $\delta^{18}O$ profile is very weak (not plotted in Fig. 3), resulting from the meltwater percolation and presumably also the fact that part of the annual layer is actually missing due to melting. However, it is interesting that the annual mean value of $\delta^{18}O$ is significantly negatively correlated with the Indian southwest monsoon (WSI1) index during 1991–2003 (Fig. 5). The WSI1 index indicates the intensity of the Indian southwest monsoon (Wang and Zhen, 1999). The correlation coefficient between the $\delta^{18}O$ time series and WSI1, –0.55, is significant at the 0.05 confidence level. In the southeastern Tibetan Plateau, the 'amount effect' of stable isotopes in summer monsoon precipitation is very significant (Araguás-Araguás and others, 1998). The more intense the Indian southwest monsoon activity, the higher the rainfall and the more depleted it is in heavy isotopes. Although the seasonal variation of $\delta^{18}O$ has been smoothed by the meltwater percolation during the summer ablation season, it is possible that the summer monsoon information can be retained by the $\delta^{18}O$ records in the firn profile. Firstly, there is net accumulation during the summer monsoon season, although summer snow ablation at the sampling site is also significant. The snow accumulated during the summer monsoon months originates from marine air masses driven by the Indian southwest monsoon, and information about summer monsoon activity must be recorded in the snow. Secondly, the meltwater itself is also tagged with the summer monsoon signal because it is mainly produced from summer snow. The $\delta^{18}O$ values in snow within a balance year must be homogenized by isotopic exchange between snow and meltwater during the meltwater percolation process. Thus it is reasonable to assume that information about the summer monsoon is recorded by the $\delta^{18}O$ values. This result indicates that reconstruction of paleo-Indian southwest monsoon activity is possible using $\delta^{18}O$ records from ice cores drilled in the monsoonal temperate-glacier area.

The reconstructed NH_4^+ concentration in the firn profile from 1991 to 2003 is shown in Figure 6. It is clear that the NH_4^+ concentration was low from 1991 to 1997, and higher from 1998 to 2003. The variation of NH_4^+ concentration seems to relate to that of WSI1 during the 1991–2003 period. Specifically, the low concentration of NH_4^+ from 1991 to 1997 corresponds to low values of the WSI1 index, while the high concentration of NH_4^+ from 1998 to 2003 is associated with high values of the WSI1 index (Figs 5 and 6). This suggests that the higher the southwest monsoon intensity, the higher the NH_4^+ concentration. It has been

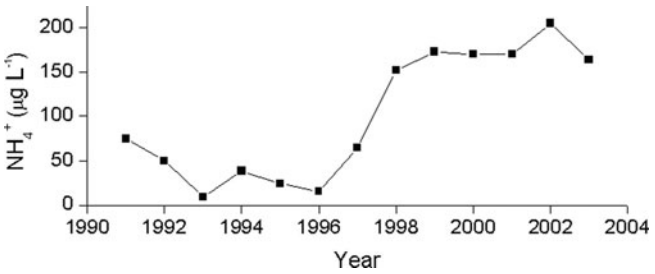

Fig. 6. Variation of the NH_4^+ concentration in the firn profile from Yulong mountain, 1991–2003.

https://doi.org/10.3189/172756407782871648 Published online by Cambridge University Press

reported that a higher proportion of NH_4^+ in snow over the high Himalaya during the summer monsoon season is linked to a stronger monsoon circulation, advecting air masses rich in NH_3 that originates from agricultural and biogenic sources in low-lying areas (Shrestha and others, 1997). A linkage between NH_4^+ in the firn profile on Yulong mountain and the Indian southwest monsoon activity is therefore possible. However, there is a need to confirm this linkage with additional data from other monsoon temperate glacier areas because post-depositional processes can also influence the ammonium concentration in snow (Sun and others, 1998).

4. CONCLUSIONS

The following conclusions can be drawn from the above analyses and discussions: (1) the chemical species in snow and firn on Yulong mountain originate from three different sources, marine, crustal and anthropogenic; (2) the variation in net accumulation of snow at Yulong mountain is controlled by temperature fluctuations and is less influenced by precipitation, probably indicating that the net accumulation is more sensitive to temperature than to precipitation in the temperate glacier area under the global warming condition; (3) although the isotopic composition is influenced significantly by post-depositional processes, especially meltwater percolation, the correlation between the WSI1 index and the $\delta^{18}O$ record of the firn profile on Yulong mountain is significant, confirming that information about past Indian southwest monsoon activity can be obtained from ice cores drilled in the monsoonal temperate-glacier area.

ACKNOWLEDGEMENTS

This research was supported by grants from the National Natural Science Foundation of China (40501014 and 90511007), funding from the orientation project of the Chinese Academy of Sciences (kzcx2-yw-317) and the fellowship project of the Chinese Academy of Sciences (0723411001). We greatly appreciate suggestions from the two anonymous referees for the improvement of our paper. We also thank M. Sharp for language editing and helpful comments and suggestions.

REFERENCES

Aizen, V., E. Aizen, J. Melack and T. Martma. 1996. Isotopic measurements of precipitation on central Asian glaciers (southeastern Tibet, northern Himalayas, central Tien Shan). *J. Geophys. Res.,* **101**(D4), 9185–9196.

Araguás-Araguás, L., K. Froelich and K. Rozanski. 1998. Stable isotope composition of precipitation over southeast Asia. *J. Geophys. Res.,* **103**(D22), 28,721–28,742.

Arndt, R.L., G.R. Carmichael and J.M. Roorda. 1998. Seasonal source–receptor relationships in Asia. *Atmos. Environ.,* **32**(8), 1397–1406.

Davidson, C.I., S. Lin, J.F. Osborn, M.R. Pandey, R.A. Rasmussen and M.A.K. Khalil. 1986. Indoor and outdoor air pollution in the Himalayas. *Environ. Sci. Technol.,* **20**(6), 561–567.

He, Y., T. Yao, G. Cheng and M. Yang. 2001. Climatic records in a firn core from an Alpine temperate glacier on Yulong mountain, southeastern part of the Tibetan Plateau. *Episodes,* **24**(1), 13–18.

He, Y., T. Yao, W.H. Theakstone, G. Cheng, M. Yang and T. Chen. 2002. Recent climatic significance of chemical signals in a shallow firn core from an alpine glacier in the South-Asia monsoon region. *J. Asian Earth Sci.,* **20**(3), 289–296.

Hou, S., D. Qin, D. Zhang, S. Kang, P.A. Mayewski and C.P. Wake. 2003. A 154 a high-resolution ammonium record from the Rongbuk Glacier, north slope of Mt. Qomolangma (Everest), Tibet–Himal region. *Atmos. Environ.,* **37**(5), 721–729.

Iizuka, Y., M. Igarashi, K. Kamiyama, H. Motoyama and O. Watanabe. 2002. Ratios of Mg^{2+}/Na^+ in snowpack and an ice core at Austfonna ice cap, Svalbard, as an indicator of seasonal melting. *J. Glaciol.,* **48**(162), 452–460.

Jang, M., N.M. Czoschke, S. Lee and R.M. Kamens. 2002. Heterogeneous atmospheric aerosol production by acid-catalyzed particle-phase reactions. *Science,* **298**(5594), 814–817.

Kang, S., C.P. Wake, D. Qin, P.A. Mayewski and T. Yao. 2000. Monsoon and dust signals recorded in Dasuopu glacier, Tibetan Plateau. *J. Glaciol.,* **46**(153), 222–226.

Koerner, R.M. 1997. Some comments on climatic reconstructions from ice cores drilled in areas of high melt. *J. Glaciol.,* **43**(143), 90–97.

Kreutz, K.J., V.B. Aizen, L.D. Cecil and C.P. Wake. 2001. Oxygen isotopic and soluble ionic composition of a shallow firn core, Inilchek glacier, central Tien Shan. *J. Glaciol.,* **47**(159), 548–554.

Li, J. and Z. Su, *eds.* 1996. *Glaciers in the Hengduanshan.* Beijing, Science Press. [In Chinese with English summary.]

Meeker, L.D., P.A. Mayewski and P. Bloomfield. 1995. A new approach to glaciochemical time series analysis. *In* Delmas, R.J., *ed. Ice core studies of global biogeochemical cycles.* Berlin, etc., Springer-Verlag, 383–400.

Nakazawa, F. *and 8 others.* 2004. Application of pollen analysis to dating of ice cores from lower-latitude glaciers. *J. Geophys. Res.,* **109**(F4), 4001. (10.1029/2004JF000125.)

Schotterer, U. *and 7 others.* 1977. Isotope measurements on firn and ice cores from alpine glaciers. *IAHS Publ.* 118 (Symposium at Grenoble 1975 – *Isotopes and Impurities in Snow and Ice*), 232–236.

Shi, Y., M. Huang and B. Ren. 1988. *An introduction to the glaciers in China.* Beijing, Chinese Academy of Science Press.

Shrestha, A.B., C. Wake and J. Dibb. 1997. Chemical composition of aerosol and snow in the high Himalaya during the summer monsoon season. *Atmos. Environ.,* **31**(17), 2815–2826.

Stichler, W., D. Baker, H. Oerter and P. Trimborn. 1982. Core drilling on Vernagtferner (Oetztal Alps, Austria) in 1979: deuterium and oxygen-18 contents. *Z. Gletscherkd. Glazialgeol.,* **18**(1), 23–35.

Su, Z. and L. Wang. 1996. Characteristics of ablation, hydrology and hydrogeochemistry of glaciers in the Hengduan mountain range. *In* Li, J. and Z. Su, *eds. Glaciers in Hengduanshan range.* Beijing, Science Press, 70–110. [In Chinese with English summary.]

Sun, J. *and 6 others.* 1998. Soluble species in aerosol and snow and their relationship at Glacier 1, Tien Shan, China. *J. Geophys. Res.,* **103**(D21), 28,021–28,028.

Wagenbach, D. 1989. Environmental records in alpine glaciers. *In* Oeschger, H. and C.C. Langway, Jr, *eds. The environmental record in glaciers and ice sheets.* Chichester, etc., John Wiley and Sons, 69–83.

Wake, C.P., P.A. Mayewski, Z. Xie, P. Wang and Z. Li. 1993. Regional distribution of monsoon and desert dust signals record in Asian glaciers. *Geophys. Res. Lett.,* **20**(14), 1411–1414.

Wang, B. and F. Zhen. 1999. Choice of South Asian summer monsoon indices. *Bull. Am. Meteorol. Soc.,* **80**(4), 629–638.

https://doi.org/10.3189/172756407782871648 Published online by Cambridge University Press